Geochronology, 7, 255–263, 2025
https://doi.org/10.5194/gchron-7-255-2025

Cosmogenic ^{3}He dating of olivine with tightly retained mantle ^{3}He, Volcano Mountain, Yukon

Jessica M. Mueller[1], Jeffrey D. Bond[2], Kenneth A. Farley[1], and Brent C. Ward[3]

[1]Division of Geological & Planetary Sciences, California Institute of Technology, Pasadena, CA 91125, USA
[2]Yukon Geological Survey, Yukon, Y1A 2C6, Canada
[3]Simon Fraser University, Burnaby, V5A 1S6, Canada

Correspondence: Jessica M. Mueller (jessica@caltech.edu)

Received: 30 May 2024 – Discussion started: 24 July 2024
Revised: 1 April 2025 – Accepted: 3 April 2025 – Published: 4 August 2025

Abstract. We present a step-heat method for isolating cosmogenic ^{3}He (^{3}He$_c$) from mantle He in olivine xenocrysts to date the eruption of four of the morphologically youngest nephelinite lava flows from Volcano Mountain (VM), the youngest cone in the Fort Selkirk volcanic field in Yukon, Canada. In these olivines, the standard procedure of powdering grains to $< 30\,\mu$m failed to effectively remove mantle helium prior to fusion: samples from four different flows yielded unusually high powder fusion ^{4}He concentrations of 1.8 to 6.3 pmol g^{-1}, with ^{3}He/^{4}He ratios of 7.9 to 9.6 R_A. When combined with the ^{3}He/^{4}He ratios obtained by crushing (average 8.1±0.2 R_A), these measurements yield Holocene cosmogenic exposure ages but with very large uncertainties arising from the large mantle ^{3}He correction. The inability to effectively isolate ^{3}He$_c$ from these samples likely arises from the survival of small ($\ll 30\,\mu$m) fluid inclusions hosting mantle He through the powdering step. The presence of such unusually small fluid inclusions may relate to the origin of the olivines as disaggregated peridotite xenoliths rather than the more commonly analyzed olivine phenocrysts. We circumvented this problem by step-heating powdered olivine in steps of 800, 1000, and 1400 °C. Helium isotopic systematics indicate that 70 %–90 % of ^{3}He$_c$ was released in the low temperature step, and the rest was released in the middle temperature step. By the highest temperature step, the released He had a mantle-like ^{3}He/^{4}He ratio. Combining results from the step-heating and crush–fusion methods, we determined that the four Volcano Mountain lava flows erupted approximately coevally, at 10.5 ± 1.7 ka.

1 Introduction

The in situ production of cosmogenic ^{3}He in olivine has been used to date the surface exposures of lava flows for decades (e.g., Aciego et al., 2007; Kurz et al., 1990; Marchetti et al., 2020). The abundance of millimeter-size olivine crystals in basalt and the high helium retentivity of olivine (Shuster and Farley, 2004; Trull and Kurz, 1993) make it an ideal candidate for cosmogenic ^{3}He dating. The method is particularly suited to the determination of eruption ages of young volcanics (Heineke et al., 2016; Fenton and Niedermann, 2014; Licciardi et al., 1999) because ^{3}He has one of the highest production / detection limit ratios amongst cosmogenic nuclides (Niedermann, 2002).

Cosmogenic ^{3}He in terrestrial rocks is primarily produced by spallation of target nuclei in the crystal lattice of minerals. At surface temperatures, ^{3}He$_c$ accumulates quantitatively in the matrix of olivine (Kurz, 1986a, b), allowing exposure ages to be obtained from independently established production rates. Unlike cosmogenic radionuclides such as ^{10}Be and ^{26}Al in which the background nuclide concentration is often negligible, a practical challenge of the ^{3}He method is isolating the cosmogenic component from other ^{3}He components. The most common non-cosmogenic sources of ^{3}He include thermal neutron capture on ^{6}Li (Andrews and Kay, 1982; nucleogenic ^{3}He, ^{3}He$_{nuc}$) and mantle He, with ^{3}He/^{4}He ratios well above crustal values trapped in fluid inclusions (Kurz, 1986a, b). U- and Th-bearing minerals also produce radiogenic ^{4}He (^{4}He$_{rad}$) through α decay. Taken together,

$$^3\mathrm{He}_{total} = {}^3\mathrm{He}_c + {}^3\mathrm{He}_m + {}^3\mathrm{He}_{nuc} \quad (1)$$

$$^4\mathrm{He}_{\mathrm{total}} = {}^4\mathrm{He}_{\mathrm{m}} + {}^4\mathrm{He}_{\mathrm{rad}}. \quad (2)$$

However, concentrations of Li, U, and Th in olivine tend to be low (Woodhead, 1996; Dostal and Capedri, 1975; Kent and Rossman, 2002; Blard and Farley, 2008; Amidon et al., 2009; Blard et al., 2013) such that neutron capture and radioactive decay produces minimal amounts of He in most young lava flows. Thus, in the specific limiting case in which nucleogenic/radiogenic He can be ignored,

$$^3\mathrm{He}_{\mathrm{total}} = {}^3\mathrm{He}_{\mathrm{c}} + {}^3\mathrm{He}_{\mathrm{m}} \quad (3)$$

$$^4\mathrm{He}_{\mathrm{total}} = {}^4\mathrm{He}_{\mathrm{m}}. \quad (4)$$

Equation (3) highlights the finding that cosmogenic ^{3}He dating in young olivine requires the isolation of $^3\mathrm{He}_{\mathrm{c}}$ from $^3\mathrm{He}_{\mathrm{m}}$. Past studies (e.g., Kurz, 1986a) achieved sufficient separation of the two components using a two-step process in which the first step is crushing whole olivine grains in vacuum and measuring the ^{3}He/^{4}He ratio. Vacuum-crushing olivine grains to $< 500\,\mu$m releases most mantle He in fluid inclusions and yields the crush ratio for a given sample, $(^3\mathrm{He}/^4\mathrm{He})_{\mathrm{crush}}$ (Kurz, 1986a, b; Puchol et al., 2017; Blard, 2021). In the second step, the crushate is powdered to reduce the number of surviving fluid inclusions and then fused in vacuum to measure mostly matrix-hosted He. In basalts, crush ratios are often close to the upper mantle ratio of ~ 8 times the atmospheric ratio ($R_{\mathrm{A}} = 1.384 \times 10^{-6}$), while fusion ratios ($(^3\mathrm{He}/^4\mathrm{He})_{\mathrm{fusion}}$) of cosmic-ray irradiated samples may be several times higher (Kurz, 1986a, b). If $^4\mathrm{He}_{\mathrm{fusion}}$ is assumed to be entirely mantle derived (Eq. 4), then the cosmogenic component can be isolated even if some of the He in the fusion is mantle derived:

$$^3\mathrm{He}_{\mathrm{c}} = {}^3\mathrm{He}_{\mathrm{fusion}} - {}^4\mathrm{He}_{\mathrm{fusion}} \times \left(\frac{^3\mathrm{He}}{^4\mathrm{He}}\right)_{\mathrm{crush}}. \quad (5)$$

$^3\mathrm{He}_{\mathrm{c}}$ is then used to calculate an exposure age. The uncertainty on $^3\mathrm{He}_{\mathrm{c}}$ depends in part on how large and how well known the correction for mantle He is. When powdering does not effectively remove the mantle component, the correction can be large compared to the total ^{3}He measurement.

In this study, we attempted the crush–fusion method to obtain exposure ages for the youngest lava flows from Volcano Mountain in Yukon, Canada; however the mantle component was so large and well retained during powdering that precise $^3\mathrm{He}_{\mathrm{c}}$ concentrations could not be obtained. As an alternative we applied a protocol previously used on cosmic-ray-exposed peridotites (Swindle et al., 2023) in which step heating successfully isolated cosmogenic ^{3}He from mantle ^{3}He.

2 Geologic setting

The Fort Selkirk volcanic complex in Yukon, Canada, is comprised of valley-filling volcanics that interacted with Cordilleran ice sheets during the Pliocene and Pleistocene epochs (Jackson et al., 2012; Jackson and Huscroft, 2023). Radiometric ages on the complex range from 0.4 to 4.3 Ma (Jackson and Huscroft, 2023). Volcano Mountain, also called *Nelruna* in the local First Nations language, is located north of the confluence of the Yukon and Pelly rivers and is the youngest volcanic center in the complex (Jackson and Stevens, 1992). It rises several hundred meters above the valley fill and is comprised of lava flows, some of very youthful appearance. Among the more recent flows are several that dammed small lakes in the Early–Middle Holocene, at some time before 7300–4200 BP (Jackson and Stevens, 1992; Francis and Ludden, 1990). The youngest flows could be even younger (Jackson and Stevens, 1992; Francis and Ludden, 1990). Jackson and Huscroft (2023) provide detailed field descriptions, photographs, and an eruptive history of Volcano Mountain.

Volcano Mountain lava flows are nephelinites carrying ultramafic xenoliths (mostly dunite) and olivine phenocrysts and xenocrysts (Francis and Ludden, 1990; Trupia and Nicholls, 1996). The xenocrysts are large (up to 1 cm) and are the dominant population of olivine crystals in the rock. Based on deformation features such as kink-banding and subgrain boundaries, their anhedral/broken shape, and highly magnesian composition (Fo88-90), they are likely disaggregated dunite xenoliths (Francis and Ludden, 1990; Trupia and Nicholls, 1996). These abundant and large xenocrysts are an attractive target for cosmogenic ^{3}He dating.

3 Samples

3.1 Field sampling

Sampling of Volcano Mountain lavas was intended to date flows of the most youthful appearance and stratigraphic position to determine the age of the most recent eruption (Table 1; Fig. 1). Particular attention was paid to the flow within the small summit crater as the most likely to be the youngest. For redundancy purposes, two to three samples were collected at each location. Site parameters used to guide sampling included a relatively flat, stable surface exhibiting primary depositional features (e.g., ropy textures) and, if possible, minimal vegetation cover. A gas-powered cutoff saw was used to control sampling by slicing the surface to a uniform depth. A rock hammer and chisel were used to liberate the sample from the prepared area. Approximately 2 kg of sample was collected from each site.

A total of 13 samples were collected on six separate lava flow surfaces. Jackson and Stevens (1992) (see also Jackson and Huscroft, 2023) mapped VM flows and named them based on the direction of the flow (north or south) and its stratigraphic position relative to the other flows based on field observations (0–2, where 2 is assigned to the youngest flows) (Fig. 1). Samples VM-01, 02, and 03 were collected from the stratigraphically highest flow in the cinder cone (flow 2Na). VM-06 is from the fifth south flow (flow 2Sa), VM-08 and 09

Table 1. Details of Volcano Mountain samples.

Flow	Sample	Latitude (N)	Longitude (W)	Elevation (m)	Depth (cm)	Shielding factor
2Na	VM-01	62.92311	137.3775	1052	3	0.96
2Na	VM-02	62.92302	137.3779	1067	3	0.96
2Na	VM-03	62.92302	137.3779	1067	3.5	0.96
2Sa	VM-06	62.90544	137.4374	718	3	0.97
1Sa	VM-08	62.90447	137.4359	725	2.5	0.96
1Sa	VM-09	62.90413	137.4368	725	2	0.96
1N	VM-10	62.95478	137.36848	788	3.5	0.98
1N	VM-11	62.9547	137.36888	785	3.5	0.97

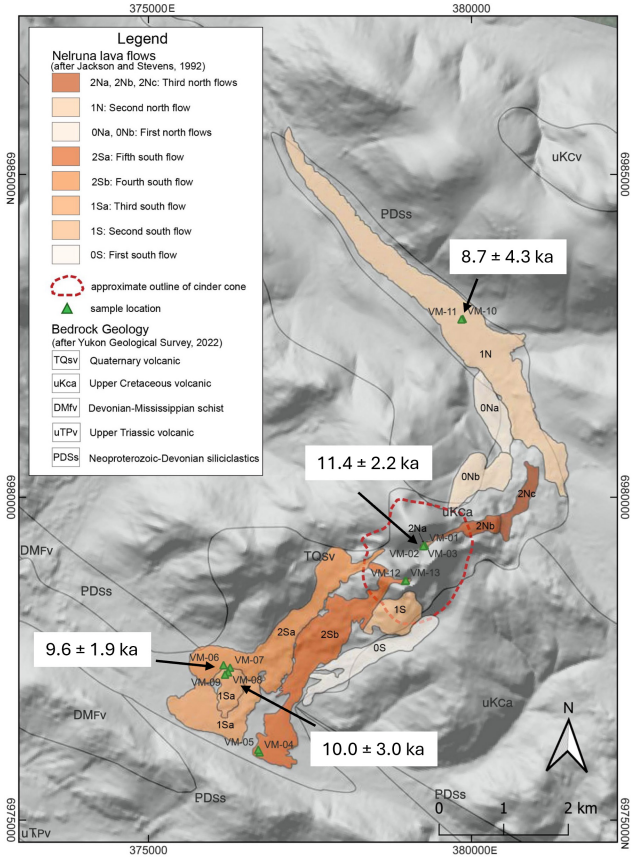

Figure 1. Geologic map of Volcano Mountain (*Nelruna*). Map of Volcano Mountain study area after Jackson and Stevens (1992). Samples VM 01, 02, and 03 are from the stratigraphically youngest flow on Volcano Mountain, while the other samples all come from flows of very youthful appearance. Numbers in boxes indicate our best estimate of eruption age based on cosmogenic ^{3}He.

are samples from the third south flow (flow 1Sa), and VM-10 and VM-11 are samples from the second north flow (flow 1N). Samples VM-04, 05, 12, and 13 are from the fourth south flow (flow 2Sb, possibly the same age as flow 2Sa, Jackson and Huscroft, 2023) but, along with sample VM-07 (flow 2Sa), yielded too little olivine to make a cosmogenic ^{3}He measurement. See Table 1 for sample details.

At elevations ranging from ∼ 0.7–1.1 km, the area experiences on average 28.8 cm of snow cover for 5.5 months of the year (Government of Canada, 2007). Vegetation, including lichen and moss, covered a significant surface area of the samples, though it is highly variable, from no coverage at VM-03 to covered in a mat of moss 8 cm thick at VM-08.

3.2 Sample selection and preparation

All hand samples were scrubbed of vegetation, rinsed in water, dried in air, and jaw-crushed to millimeter-sized grains. The abundance of coarse olivine crystals varied among samples; only samples VM-01, 02, 03, 06, and 08 through 11 had sufficient olivine for cosmogenic ^{3}He measurement. From these, matrix-free, millimeter-size olivine crystals were handpicked from the crushate based on their distinct lack of cleavage and green color.

4 Analytical methods

4.1 Crushing and powder fusion method

Helium was extracted from olivines by crushing under vacuum for 2 min and then re-crushed for another 5 min. The two steps were combined into a single He result. Previous work with this same crusher design indicates these crush durations will not cause release of matrix-sited ^{3}He (Blard et al., 2008). Prior to dropping samples into the crusher anvil, 2 min "no sample" crushes were measured and used to blank-correct He measurements. Maximum blank crush levels of ^{3}He and ^{4}He were 2000 atoms and 0.009 pmol, respectively.

For some samples, material recovered from the vacuum crushes was powdered in a mortar and pestle under ethanol and sieved to $< 30\,\mu m$, dried, weighed, and wrapped in Sn foil packets for fusion analysis. For other samples analyzed by fusion, the handpicked olivines did not undergo the initial vacuum-crush step, only powdering under ethanol. Ethanol was used to circumvent (Cox et al., 2022) trapping of atmospheric He during powdering (Protin et al., 2016).

Sn-foil-wrapped samples for high temperature vacuum extraction analysis were loaded into the dropper arm of a double-wall furnace and evacuated overnight. The dropper arm was not heated to eliminate any possibility of baking-induced loss of ^{3}He. The furnace was outgassed directly into the vacuum pump for 1 h at 1400 °C prior to analysis. Samples were then dropped into a carbon liner in the furnace and heated to ~ 1200 °C for 25 min. Re-extracts were measured directly after each extraction to ensure the complete release of helium. When the re-extract signal exceeded the pre-analysis hot blank, the re-extract was repeated. All sample gas in excess of blank was combined in the concentrations reported here. While these olivines were not fused during these analyses (the temperature was held sub-melting to minimize He blanks), complete He extraction is ensured by the re-extraction steps. For consistency with prior work, we nevertheless refer to these measurements as "powder fusions". Two olivine samples were fused in a lithium borate flux at ~ 1000 °C for 25 min in a molybdenum liner. The flux was used in these fusions to reduce blank He levels by lowering extraction temperature (Farley et al., 2020). Hot blanks at ~ 1200 °C for ^{3}He and ^{4}He were 22 000 atoms and 0.009 pmol, respectively. Blanks measured on the tin foil are negligible compared to this hot furnace blank. Blank corrections made to sample gas concentrations were mostly $< 2\,\%$ but always $< 5\,\%$.

4.2 Step heating

About 750 mg of powdered ($< 30\,\mu m$) sample was wrapped in Sn foil packets and loaded into the vacuum furnace as described above. The Sn packets were then dropped into the furnace and He successively released at 800, 1000, and 1400 °C each for 30 min duration. These temperature steps were selected based on previous studies reporting the release of cosmogenic ^{3}He below 1000 °C (Kurz, 1986a; Swindle et al., 2023). A thermocouple and a pyrometer were used to calibrate furnace temperatures as a function of furnace output power, after which heating steps were maintained using constant power output.

Hot blanks were performed on an empty furnace at each of the scheduled temperature steps to use as blank corrections on He quantities at each step. Blank levels were $< 1.5\,\%$ of extracted He for all steps. Re-extracts were measured on the material after step heating to ensure total helium release. When the re-extract signal exceeded the pre-analysis hot blank, the re-extract was repeated. When the re-extract exceeded the hot blank, the excess He was added to the high temperature step.

4.3 Helium measurement

Helium was purified and measured as previously described (Horton et al., 2019; Swindle et al., 2023). Gas extracted from the furnace was passed through a charcoal U-trap to remove contaminants such as CO_2, H_2O, and Ar. Remaining reactive gases were removed using a hot SAES NP10 getter, and H_2 was removed using a cold SAES NP10 getter. Helium was then cryofocused on charcoal at 14 K and released at 34 K into a Helix SFT mass spectrometer. ^{3}He was measured on a pulse-counting electron multiplier and ^{4}He on a Faraday cup. Instrument sensitivity and internal consistency were monitored by running a standard containing ~ 3.1 pmol of He (^{3}He/^{4}He ratio $= 2.05\ R_A$) throughout our experiments. This standard was created from pure ^{3}He and ^{4}He using a capacitance manometer, and the amounts delivered are known to better than $\pm 1\,\%$.

4.4 Shielding correction

Corrections for snow cover, vegetation cover, and self-shielding were considered for every sample. The snow correction factor was calculated using Eq. (3) in Vermeesch (2007) based on the spallogenic neutron attenuation length, average snow thickness, and snow density. A snow density of $0.3\ g\,cm^{-3}$ was assumed. Topographic shielding corrections were made for VM-01, 02, and 03 due to their location inside the VM cinder cone (see red outline in Fig. 1). Topographic shielding for the other samples was negligible. Shielding factors are listed in Table 1.

5 Results

5.1 Crush and fusion results

Analytical results for the crushing and fusion experiments are listed in Table 2. The three samples (VM-02, VM-06, and VM-09) analyzed by crushing come from three different flows (2Na, 2Sa, and 1Sa) yet have indistinguishable crush ^{3}He/^{4}He ratios (7.99 ± 0.19, 8.08 ± 0.19, and $8.23 \pm 0.2\ R_A$). Crush-release He concentrations in these samples are high for basalt-hosted olivines, ranging from 3.38 to $8.20\ pmol\ g^{-1}$.

Six powder fusion analyses and the total helium yield from the three step heats (described below) provide information on the matrix-hosted helium in all four of the investigated lava flows. Across these nine analyses, He concentrations range from 1.74 to $6.30\ pmol\ g^{-1}$, similar to the crush results. ^{3}He/^{4}He ratios ranged from 7.9 ± 0.2 to $9.6 \pm 0.2\ R_A$. For the three lava flows for which both crushing and fusion analyses are available, fusion ^{3}He/^{4}He ratios ranged from the same

Table 2. Helium isotope data on samples analyzed by crushing and bulk fusion. Also included are total yields from step-heating experiments in Table 3.

Flow	Sample	Analysis type	Mass g	^{3}He Mat g^{-1}	±	^{4}He pmol g^{-1}	±	^{3}He/^{4}He R_A	±	^{3}He$_c$ Mat g^{-1}	±	^{3}He$_c$ %
2Na	VM-02	Crush	0.097	54.9	1.1	8.20	0.16	7.99	0.19			
2Na	VM-02	Fusion	0.246	35.3	0.7	4.86	0.10	8.67	0.25	2.75	1.25	7.8
2Na	VM-01	StepHt	0.734	30.5	1.1	4.06	0.14	8.96	0.26	3.27	1.57	10.8
2Na	VM-03	StepHt	0.800	35.4	1.2	4.68	0.16	9.03	0.25	4.05	1.82	11.4
2Sa	VM-06	Crush	0.630	22.8	0.5	3.38	0.04	8.08	0.19			
2Sa	VM-06	Fusion	0.500	13.8	0.3	1.72	0.03	9.59	0.27	2.19	0.36	15.8
1Sa	VM-09	Crush	0.100	32.7	0.7	4.75	0.06	8.23	0.20			
1Sa	VM-09	Fusion	0.068	13.7	1.0	2.06	0.08	7.94	0.71	−0.51	1.16	
1Sa	VM-08	Fusion	0.320	18.7	0.4	2.38	0.05	9.37	0.27	2.27	0.64	12.1
		Assumes average of all VM crushes:						8.10	0.20			
1N	VM-10	Fusion	0.116	14.8	1.1	2.12	0.04	8.36	0.33	0.46	1.17	3.1
1N	VM-11	Fusion	0.100	30.9	0.6	4.48	0.09	8.25	0.24	0.56	1.15	1.8
1N	VM-11	StepHt	0.657	44.3	1.5	6.28	0.22	8.44	0.41	1.79	2.37	4.0

within error as the crush result (VM-09 from flow 1Sa), to a maximum of 1.5 R_A higher (VM-06 from flow 2Sa).

We used these data to compute cosmogenic ^{3}He concentrations via Eq. (1) by assuming that the crush ^{3}He/^{4}He ratio on a given flow can be applied to all samples obtained from that flow. For flow 1N, for which we did not measure a sample by crushing, we computed cosmogenic ^{3}He concentrations by assuming the mean crush ^{3}He/^{4}He ratio of 8.1 ± 0.2 R_A obtained on the other flows. This assumption is supported by the step-heat results described below.

Cosmogenic ^{3}He was confidently detected in five of the nine fusion analyses (Table 3). For flow 2Na we obtained cosmogenic ^{3}He concentrations of 2.75 ± 1.25 Mat g^{-1} (VM-02), 3.27 ± 1.57 Mat g^{-1} (VM-01), and 4.05 ± 1.82 Mat g^{-1} (VM-03). One analysis each of flow 2Sa (VM-06) and 1Sa (VM-08) yielded ^{3}He$_c$ of 2.19 ± 0.36 and 2.27 ± 0.64 Mat g^{-1}, respectively. For the remaining four analyses the 1σ analytical uncertainty on ^{3}He$_c$ exceeds the measured value; i.e., the cosmogenic ^{3}He concentration is indistinguishable from zero.

The high analytical uncertainties on ^{3}He$_c$ – typically more than 1 Mat g^{-1} – in the VM samples arise from the large corrections required for mantle ^{3}He present in the powder fusion analyses (Eq. 1). For example, as shown in Table 2, the fraction of ^{3}He that is cosmogenic in these analyses ranges from a maximum of 15.8 % (VM-06) to < 2 % (VM-11, VM-09). Stated differently, the ^{3}He/^{4}He ratios obtained by fusion are very close to the ratios obtained by crushing, and this similarity at least in part reflects preservation of a high concentration of mantle helium through the powdering step.

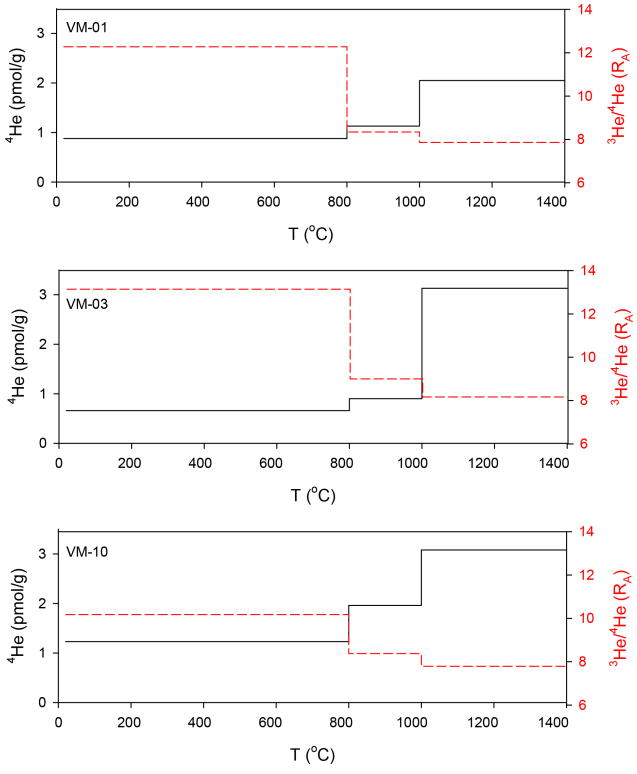

Figure 2. Step-heat results on three Volcano Mountain samples. Samples were analyzed at three successive temperatures (800, 1000, and 1400 °C) held for 30 min each. Horizontal lines indicate the temperature range over which each measurement integrates. The dashed red line indicates the ^{3}He/^{4}He ratio (right-hand axis), while the solid black line indicates the ^{4}He concentration (left-hand axis).

Table 3. Helium isotope data on samples analyzed by step heating. Only the first two steps contain cosmogenic ^{3}He.

Flow	Sample	Mass g	Step	^{3}He Mat g^{-1}	±	^{4}He pmol g^{-1}	±	^{3}He/^{4}He R_A	±	^{3}He$_c$ Mat g^{-1}	±	^{3}He$_c$ %
2Na	VM-01	0.734	800	9.14	0.27	0.88	0.02	12.3	0.35	3.26	0.27	36.0
			1000	7.79	0.27	1.13	0.02	8.35	0.24	0.45	0.30	5.8
			1400	13.4	0.27	2.05	0.04	7.87	0.22			
			Total	30.4	1.1	4.06	0.14	8.96	0.44			
			Total cosmogenic							3.71	0.41	
2Na	VM-03	0.800	800	7.26	0.27	0.66	0.01	13.14	0.37	2.76	0.21	37.9
			1000	6.72	0.27	0.90	0.02	9.00	0.26	0.62	0.25	9.3
			1400	21.2	0.54	3.13	0.06	8.17	0.23			
			Total	35.5	0.80	4.68	0.01	9.03	0.44			
			Total cosmogenic							3.38	0.33	
1N	VM-10	0.657	800	10.5	0.27	1.23	0.03	10.18	0.29	2.47	0.35	23.5
			1000	13.7	0.27	1.96	0.04	8.38	0.24	0.97	0.52	7.0
			1400	20.2	0.27	3.08	0.06	7.79	0.22			
			Total	44.3	1.6	6.28	0.22	8.44	0.41			
			Total cosmogenic							3.43	0.63	

5.2 Step heat

Because the crush–fusion method was not especially successful in isolating the cosmogenic component, we attempted step heating on two samples from the stratigraphically youngest flow (2Na, samples VM-01 and VM-03) and one from the stratigraphically oldest flows (Flow 1N, sample VM-10). Results are shown in Table 3 and Fig. 2. In all three samples, the ^{3}He/^{4}He ratios decline monotonically with extraction temperature, while the ^{4}He yields increase. For example, in sample VM-03, the 800, 1000, and 1400 °C steps yielded ^{3}He/^{4}He ratios of 13.1, 9.0, and 8.2 R_A and ^{4}He concentrations of 0.67, 0.89, and 3.1 pmol g^{-1}, respectively. Previous work indicates that mantle He in fluid inclusions is released at extraction temperatures > 1000 °C (Kurz, 1986a, b; Swindle et al., 2023). In the case of the VM samples, the ^{3}He/^{4}He ratios extracted in the final steps (7.87 ± 0.22, 8.17 ± 0.23, 7.79 ± 0.22 R_A) are indistinguishable from the mean ^{3}He/^{4}He ratio obtained by crushing (8.10 ± 0.20 R_A), supporting this conclusion.

6 Discussion

6.1 Tightly retained mantle He in Volcano Mountain olivine

^{3}He/^{4}He ratios of He released by crushing and in the highest temperature step of the step heats are within the typical range of mid-ocean ridge basalts (Graham et al., 1992), suggesting He in Volcano Mountain derives from the upper mantle. Regardless of its origin, the presence of this mantle He substantially complicates determination of cosmogenic ^{3}He exposure ages. While mantle ^{4}He concentrations of crushed olivines are sometimes, but not often (Kurz et al., 1990; Farley and Neroda, 1998; Fenton and Niedermann, 2014; Heineke et al., 2016), as high as the ∼ 4.5 pmol g^{-1} we obtained on the VM samples, the more important complication arises from the fact that this mantle He is not effectively removed by powdering to < 30 µm. Our powder fusion analyses indicate that about a third of the mantle component remains in the powdered olivine in every case. Our results suggest a mantle component that survives the powdering step, most likely in ≪ 30 µm fluid inclusions. Evidence to support this interpretation comes from our observation of trails of circular voids (< 10 µm) present in backscatter electron images of VM olivine xenocrysts. We interpret these to be secondary inclusion trails that carry mantle He. Survival of the mantle component when crushing this fine is not typical, but it is similar to results obtained on Twin Sisters peridotites (Swindle et al., 2023). Another possibility is that the ubiquitous kink banding and subgrain boundaries observed in VM (Francis and Ludden, 1990) and Twin Sisters olivines (Swindle et al., 2023) could contribute to mantle He retention.

6.2 Component separation by step heating

The step-heat method takes advantage of the different release kinetics of matrix-sited and fluid-inclusion-sited He. Diffusion alone is adequate to release matrix-sited helium; in contrast, for fluid inclusion helium to escape the crystal requires it to first dissolve into the olivine, an energetically disfavored

Table 4. Cosmogenic helium ages. C/F: crush–fusion method. StepHt: step-heating method using only the first two heating steps; see Table 3. Cosmogenic He ages are in bold.

Flow	Sample	Method	^3He_c Mat g^{-1}	±	Exp age ka	±
2Na	VM-01	C/F	2.75	1.25	9.0	4.2
	VM-02	C/F	3.27	1.57	10.8	5.3
	VM-03	C/F	4.05	1.82	13.3	6.1
	VM-01	StepHt	3.71	0.41	12.3	1.9
	VM-03	StepHt	3.38	0.33	11.1	1.6
	Weighted mean				**11.4**	**2.2**
2Sa	VM-06	C/F	2.19	0.36	**9.6**	**1.9**
1Sa	VM-08	C/F	2.27	0.64	**10.0**	**3.0**
1N	VM-10	C/F	0.46	1.17	1.9	4.8
	VM-11	C/F	0.56	1.15	2.3	4.8
	VM-11	C/F	1.79	2.37	7.4	9.9
	VM-10	StepHt	3.43	0.63	14.0	3.0
	Weighted mean				**8.7**	**4.3**

process (Trull and Kurz, 1993). Three temperature steps allowed us to be flexible about the temperature that best separates these two components. The evolution of the ^{3}He/^{4}He ratio with temperature thus can reveal two-end-member mixing between mantle and cosmogenic He (assuming radiogenic helium and nucleogenic helium are both absent).

Compared to the ^{3}He/^{4}He ratios obtained on powder fusions, the ^{3}He/^{4}He ratios of the lowest temperature steps in our step-heat experiments are between 1.5 and 4 R_A higher (Tables 2, 3). In contrast, ^{3}He/^{4}He ratios of the 1000 °C steps are very similar to the powder fusion values, and about 0.7 R_A higher than the highest temperature steps and the associated crush-released ^{3}He/^{4}He ratios. These data provide support for the interpretation that all cosmogenic He is released prior to the highest temperature step, while mantle He is released in progressively greater amounts as step temperature increases.

To calculate the cosmogenic ^{3}He concentration from the step-heat results for each sample, we assumed the final step represents the mantle component, used Eq. (1) to compute the cosmogenic ^{3}He yield in the two lower temperature steps, and combined them to obtain a total. Using this method, we obtained indistinguishable ^3He_c concentrations on the two samples of flow 2Na (3.71 ± 0.41 and 3.38 ± 0.33 Mat g^{-1}) and 3.43 ± 0.63 Mat g^{-1} on flow 1N. While still uncertain (average ±13 %), these cosmogenic concentrations are significantly better determined than by the crush–fusion method.

It is possible that a more detailed step heat could yield even greater degrees of separation between cosmogenic and mantle helium components but at the potential cost of analytical precision associated with averaging multiple analyses and with blank corrections. Were significant amounts of radiogenic and/or nucleogenic helium present in these samples (unlikely given the eruption age of ∼ 10 kyr; see below), this method would yield inaccurate results in the same way that the crush–fusion method would.

6.3 ^3He_c exposure ages

Exposure ages in Table 4 were computed from ^3He_c concentrations and corresponding uncertainties using the CRONUS-Earth online calculator (Balco et al., 2008; Phillips et al., 2016; version 3), where the production rate of ^3He_c is calibrated using data from Borchers et al. (2016). Exposure ages were obtained for four of the flows. By far the best determined is the exposure age of the youngest flow, 2Na. The two step-heat analyses (VM-01, 03) yield indistinguishable ages of 12.3 ± 1.9 and 11.1 ± 1.6 ka. These are in good agreement with the three crush–fusion pairs (VM-01, 02, 03), with ages ranging from 9.0 ± 4.2 to 13.3 ± 6.1 ka. Assuming independent uncertainties among these analyses, the weighted means of these five ages is 11.4 ± 2.2 ka (MSWD (mean square weighted distribution) 0.17, 95 %), slightly more uncertain than the step-heat analyses on their own. Four analyses were performed on flow 1N, with the step-heat experiment yielding an age of 14.0 ± 3.0 ka and three crush–fusion pairs yielding ages between 2.3 ± 4.8 and 7.4 ± 9.9 ka. The weighted mean of these analyses is 8.7 ± 4.3 ka (MSWD 2.3, 7.4 %), again more uncertain than the step-heat analysis by itself. The individual crush–fusion analyses of flows 2Sa and 1Sa yielded exposure ages of 9.6 ± 1.9 ka and 10.0 ± 3 ka, respectively.

Exposure ages are indicated on the map in Fig. 1 using the weighted means when available. All four flows yield the same exposure age within error (weighted mean of all analyses: 10.5 ± 1.7 ka, MSWD 0.92, 51 %), and there is no indication that the stratigraphically lower flows (1Sa and 1N, weighted mean 9.2 ± 3.5 ka, MSWD 1.8, 13 %) have older exposure than the higher flows (2Na and 2Sa, weighted mean 11.0 ± 1.9 ka, MSWD 0.28, 93 %).

The simplest interpretation of these results is that all of the studied VM lava flows erupted at 10.5 ± 1.7 ka. Alternatively, honoring the stratigraphy, the flows may have erupted over an age range from about 12.7 ka (1S flows) to about 9.1 ka (2Na and 2Sa).

7 Conclusion

Volcano Mountain nephelinites contain olivine likely sourced from disaggregated peridotite xenoliths. This olivine contains high concentrations of upper mantle He, and powdering does not effectively remove this component. Swindle et al. (2023) were similarly unable to remove mantle He components by powdering olivine from the Twin Sisters peridotite. In both cases, this mantle He may be housed in fluid inclusions too small to be released by crushing. Alter-

natively, ubiquitous kink bands and subgrain boundaries seen in the Twin Sisters and Volcano Mountain flows could be the source of the He that survives powdering. In either case, survival of mantle He in VM powder fusions caused the crush–fusion method to yield imprecise ^3He_c concentrations. Using the step-heating method described here, we were able to determine that the morphologically youngest lava flows on Volcano Mountain erupted approximately coevally in the earliest Holocene, 10.5 ± 1.7 ka.

Data availability. All data are provided in the figures and tables of this paper.

Author contributions. JMM prepared the manuscript with significant contributions from KAF and JDB. JDB and BCW completed the field sampling.

Competing interests. The contact author has declared that none of the authors has any competing interests.

Disclaimer. Publisher's note: Copernicus Publications remains neutral with regard to jurisdictional claims made in the text, published maps, institutional affiliations, or any other geographical representation in this paper. While Copernicus Publications makes every effort to include appropriate place names, the final responsibility lies with the authors.

Acknowledgements. We respectfully acknowledge and thank the Selkirk First Nation (SFN) for their support and guidance on this project. Roger Alfred and Elli Marcotte (SFN) provided traditional knowledge of *Nelruna* while in the field, which enlightened and guided our efforts. Sampling assistance was provided by Leyla Weston (YGS), Keyshawn Sawyer (SFN), and Sofia Bond (YGS). Funding for the fieldwork was provided by the Yukon Geological Survey. Safe access to the area was provided by Malcolm Turnbull from Capital Helicopters. We would like to thank Dale and Sue Bradley from Pelly Ranch for their hospitality while completing the fieldwork. We thank Pierre-Henri Blard and Julien Amalberti for their reviews. This paper is assigned Yukon Geological Survey contribution number 066.

Review statement. This paper was edited by Greg Balco and reviewed by David Marchetti, Julien Amalberti, and Pierre-Henri Blard.

References

Aciego, S. M., DePaolo, D. J., Kennedy, B. M., Lamb, M. P., Sims, K. W. W., and Dietrich, W. E.: Combining [He-3] cosmogenic dating with U-Th/He eruption ages using olivine in basalt, Earth Planet. Sc. Lett., 254, 288–302, 2007.

Amidon, W. H., Rood, D. H., and Farley, K. A.: Cosmogenic He-3 and Ne-21 production rates calibrated against Be-10 in minerals from the Coso volcanic field, Earth Planet. Sc. Lett., 280, 194–204, https://doi.org/10.1016/j.epsl.2009.01.031, 2009.

Andrews, J. N. and Kay, R. L. F.: Natural production of tritium in permeable rocks, Nature, 298, 361–363, 1982.

Balco, G., Stone, J. O., Lifton, N. A., and Dunai, T. J.: A complete and easily accessible means of calculating surface exposure ages or erosion rates from Be-10 and Al-26 measurements, Quat. Geochronol., 3, 174–195, 2008.

Blard, P.-H.: Cosmogenic 3He in terrestrial rocks: A review, Chem. Geol., 586, 120543, https://doi.org/10.1016/j.chemgeo.2021.120543, 2021.

Blard, P.-H. and Farley, K. A.: The influence of radiogenic ^{4}He on cosmogenic ^{3}He determinations in volcanic olivine and pyroxene, Earth Planet. Sc. Lett., 276, 20–29, https://doi.org/10.1016/j.epsl.2008.09.003, 2008.

Blard, P. H., Puchol, N., and Farley, K. A.: Constraints on the loss of matrix-sited helium during vacuum crushing of mafic phenocrysts, Geochim. Cosmochim. Ac., 72, 3788–3803, https://doi.org/10.1016/j.gca.2008.05.044, 2008.

Blard, P.-H., Braucher, R., Lavé, J., and Bourlès, D.: Cosmogenic ^{10}Be production rate calibrated against 3He in the high Tropical Andes (3800–4900 m, 20–22° S), Earth Planet. Sc. Lett., 382, 140–149, https://doi.org/10.1016/j.epsl.2013.09.010, 2013.

Borchers, B., Marrero, S., Balco, G., Caffee, M., Goehring, B., Lifton, N., Nishiizumi, K., Phillips, F., Schaefer, J., and Stone, J.: Geological calibration of spallation production rates in the CRONUS-Earth project, Quaternary Geochronol., 31, 188–198, https://doi.org/10.1016/j.quageo.2015.01.009, 2016.

Cox, S. E., Miller, H. B. D., Hofmann, F., and Farley, K. A.: Short communication: Mechanism and prevention of irreversible trapping of atmospheric He during mineral crushing, Geochronology, 4, 551–560, https://doi.org/10.5194/gchron-4-551-2022, 2022.

Dostal, J. and Capedri, S.: Partition coefficients of uranium for some rock-forming minerals, Chem. Geol., 15, 285–294, https://doi.org/10.1016/0009-2541(75)90038-8, 1975.

Farley, K. A. and Neroda, E.: Noble gases in the Earth's mantle, Annu. Rev. Earth Planet. Sci., 26, 189–218, 1998.

Farley, K. A., Treffkorn, J., and Hamilton, D.: Isobar-free neon isotope measurements of flux-fused potential reference minerals on a Helix-MC-Plus mass spectrometer, Chem. Geol., 537, 119487, https://doi.org/10.1016/j.chemgeo.2020.119487, 2020.

Fenton, C. R. and Niedermann, S.: Surface exposure dating of young basalts (1–200 ka) in the San Francisco volcanic field (Arizona, USA) using cosmogenic 3He and 21Ne, Quat. Geochronol., 19, 87–105, https://doi.org/10.1016/j.quageo.2012.10.003, 2014.

Francis, D. and Ludden, J.: The Mantle Source for Olivine Nephelinite, Basanite, and Alkaline Olivine Basalt at Fort Selkirk, Yukon, Canada, J. Petrol., 31, 371–400, https://doi.org/10.1093/petrology/31.2.371, 1990.

Government of Canada: Yukon Snow Survey Network, Historical snow and water supply data, Government of Canada [data set], https://open.yukon.ca/data/datasets/yukon-snow-survey-network/resource/ddc09d23-02f5-48b4-9635-338b89ea7a02 (last access: 13 December 2024), 2007.

Graham, D. W., Jenkins, W. J., Schilling, J. G., Thompson, G., Kurz, M. D., and Humphris, S. E.: Helium isotope geochemistry of mid-ocean ridge basalts from the South Atlantic, Earth Planet. Sc. Lett., 110, 133–148, 1992.

Heineke, C., Niedermann, S., Hetzel, R., and Akal, C.: Surface exposure dating of Holocene basalt flows and cinder cones in the Kula volcanic field (Western Turkey) using cosmogenic ^{3}He and ^{10}Be, Quat. Geochronol., 34, 81–91, https://doi.org/10.1016/j.quageo.2016.04.004, 2016.

Horton, F., Farley, K., and Jackson, M.: Helium distributions in ocean island basalt olivines revealed by X-ray computed tomography and single-grain crushing experiments, Geochim. Cosmochim. Ac., 244, 467–477, https://doi.org/10.1016/j.gca.2018.10.013, 2019.

Jackson, L. E. and Huscroft, C. A.: Eruptive history of the Fort Selkirk Area, Central Yukon, Can. J Earth Sci., 60, 1265–1282, https://doi.org/10.1139/cjes-2022-0124, 2023.

Jackson, L. E. and Stevens, W.: A recent eruptive history of Volcano Mountain, Yukon Territory, Natural Resources Canada, https://doi.org/10.4095/132784, 1992.

Jackson, L. E., Nelson, F. E., Huscroft, C. A., Villeneuve, M., Barendregt, R. W., Storer, J. E., and Ward, B. C.: Pliocene and Pleistocene volcanic interaction with Cordilleran ice sheets, damming of the Yukon River and vertebrate Palaeontology, Fort Selkirk Volcanic Group, west-central Yukon, Canada, Quaternary Int., 260, 3–20, https://doi.org/10.1016/j.quaint.2011.08.033, 2012.

Kent, A. J. R. and Rossman, G. R.: Hydrogen, lithium, and boron in mantle-derived olivine: The role of coupled substitutions, Am. Mineral., 87, 1432–1436, https://doi.org/10.2138/am-2002-1020, 2002.

Kurz, M. D.: Cosmogenic helium in a terrestrial igneous rock, Nature, 320, 435–439, 1986a.

Kurz, M. D.: In situ production of terrestrial cosmogenic helium and some applications to geochronology, Geochim. Cosmochim. Ac., 50, 2855–2862, 1986b.

Kurz, M. D., Colodner, D., Trull, T. W., Moore, R. B., and Obrien, K.: Cosmic-ray exposure dating with in-situ produced cosmogenic ^{3}He results from young Hawaiian lava flows, Earth Planet. Sc. Lett., 97, 177–189, 1990.

Licciardi, J., Kurz, M. D., Clark, P., and Brook, E.: Calibration of cosmogenic ^{3}He production rates from Holocene lava flows in Oregon, USA, and effects of the Earth's magnetic field, Earth Planet. Sc. Lett., 172, 261–271, 1999.

Marchetti, D. W., Stork, A. L., Solomon, D. K., Cerling, T. E., and Mace, W.: Cosmogenic 3He exposure ages of basaltic flows from Miller Knoll, Panguitch Lake, Utah: Using the alternative isochron approach to overcome low-gas crushes, Quat. Geochronol., 55, 101035, https://doi.org/10.1016/j.quageo.2019.101035, 2020.

Niedermann, S.: Cosmic-ray-produced noble gases in terrestrial rocks: Dating tools for surface processes, in: Noble gases in geochemistry and cosmochemistry, vol. 47, edited by: Porcelli, D., Ballentine, C. J., and Wieler, R., Mineralogical Society of America, Washington D.C., 844, https://doi.org/10.2138/rmg.2002.47.16, 2002.

Phillips, F. M., Argento, D. C., Balco, G., Caffee, M. W., Clem, J., Dunai, T. J., Finkel, R., Goehring, B., Gosse, J. C., Hudson, A. M., Jull, A. J. T., Kelly, M. A., Kurz, M., Lal, D., Lifton, N., Marrero, S. M., Nishiizumi, K., Reedy, R. C., Schaefer, J., Stone, J. O. H., Swanson, T., and Zreda, M. G.: The CRONUS-Earth Project: A synthesis, Quat. Geochronol., 31, 119–154, https://doi.org/10.1016/j.quageo.2015.09.006, 2016.

Puchol, N., Blard, P.-H., Pik, R., Tibari, B., and Lavé, J.: Variability of magmatic and cosmogenic 3 He in Ethiopian river sands of detrital pyroxenes: Impact on denudation rate determinations, Chem. Geol., 448, 13–25, https://doi.org/10.1016/j.chemgeo.2016.10.033, 2017.

Protin, M., Blard, P.-H., Marrocchi, Y., and Mathon, F.: Irreversible adsorption of atmospheric helium on olivine: A lobster pot analogy, Geochim. Cosmochim. Ac., 179, 76–88, https://doi.org/10.1016/j.gca.2016.01.032, 2016.

Shuster, D. L. and Farley, K. A.: ^{4}He/^{3}He thermochronometry, Earth Planet. Sc. Lett., 217, 1–17, https://doi.org/10.1016/S0012-821X(03)00595-8, 2004.

Swindle, C., Clark, D., and Farley, K. A.: Helium isotope evidence for mixing of mantle-derived fluids and deeply penetrating surface waters in an obducted peridotite massif, Geochim. Cosmochim. Ac., 353, 45–60, https://doi.org/10.1016/j.gca.2023.05.015, 2023.

Trull, T. W. and Kurz, M. D.: Experimental measurements of 3He and 4He mobility in olivine and clinopyroxene at magmatic temperatures, Geochim. Cosmochim. Ac., 57, 1313–1324, https://doi.org/10.1016/0016-7037(93)90068-8, 1993.

Trupia, S. and Nicholls, J.: Petrology of Recent lava flows, Volcano Mountain, Yukon Territory, Canada, Lithos, 37, 61–78, https://doi.org/10.1016/0024-4937(95)00024-0, 1996.

Vermeesch, P.: CosmoCalc: An Excel add-in for cosmogenic nuclide calculations, Geochem. Geophys. Geosyst., 8, Q08003, https://doi.org/10.1029/2006GC001530, 2007.

Woodhead, J. D.: Extreme HIMU in an oceanic setting: the geochemistry of Mangaia Island (Polynesia), and temporal evolution of the Cook—Austral hotspot, J. Volcanol. Geoth. Res., 72, 1–19, https://doi.org/10.1016/0377-0273(96)00002-9, 1996.